2013

Linear Compressors for Electronics Cooling: Energy Recovery and the Useful Benefits

C. R. Bradshaw

E. A. Groll
Purdue University

Suresh V. Garimella
Purdue Univ, sureshg@purdue.edu

Bradshaw, C. R.; Groll, E. A.; and Garimella, Suresh V., "Linear Compressors for Electronics Cooling: Energy Recovery and the Useful Benefits" (2013). *CTRC Research Publications.* Paper 204.
http://dx.doi.org/http://dx.doi.org/10.1016/j.ijrefrig.2013.02.002

Linear Compressors for Electronics Cooling: Energy Recovery and its Benefits

Craig R. Bradshaw[a], Eckhard A. Groll[b,c,1], Suresh V. Garimella[c]

[a]*Torad Engineering, Alpharetta, GA 30004*
[b]*Herrick Laboratories, Purdue University, West Lafayette, IN 47907*
[c]*Cooling Technologies Research Center, Purdue University, West Lafayette, IN 47907*

Abstract

A comprehensive model of a linear compressor for electronics cooling was previously presented by Bradshaw et al. (2011) then enhanced and used for a sensitivity analysis of the leakage gap, eccentricity, and piston geometry by Bradshaw et al. (2012). The current work utilizes the previously developed model to explore the energy recovery characteristics of a linear compressor as compared to those of a reciprocating compressor. The impact of dead (clearance) volume on both a linear and reciprocating compressor is analyzed. In contrast to a reciprocating compressor the overall isentropic efficiency of the linear compressor remains relatively unaffected by an increase in dead volume up to a certain point. This behavior is attributed to the ability of the linear compressor to recapture the energy of the compressed gas during the expansion process. This characteristic behavior allows a linear compressor to be used for efficient capacity control from roughly 35 to 100%.

Keywords: linear compressor, reciprocating compressor, capacity control, electronics cooling

[1]Corresponding Author, groll@purdue.edu ph. 1-765-496-2201, fax 1-765-494-0787

Nomenclature

A	Area	[m^2]
c_{eff}	Effective damping factor	[N sec m^{-1}]
COP	Coefficient of Performance	[-]
COP_{carnot}	Coefficient of Performance for Carnot cycle	[-]
D_p	Piston diameter	[m]
F_{drive}	Driving force	[N]
F_{gas}	Force applied by gas	[N]
f	Dry friction coefficient	[-]
g	Leakage gap between piston and cylinder	[μm]
h	Enthalpy	[kJ kg^{-1}]
J	Moment of inertia	[kg-m]
k_{gas}	Stiffness from gas	[N m^{-1}]
k_{mech}	Mechanical stiffness	[N m^{-1}]
L	Length	[m]
$\dot{m}$	Massflow rate	[kg s^{-1}]
M_{mov}	Moving mass	[kg]

N	Normal force from piston to cylinder	[N]
n	Polytropic exponent	[-]
P	Pressure	[kPa]
$\dot{Q}_{cool}$	Cooling capacity	[W]
r	Radius	[m]
T	Temperature	[K]
T	Torque	[N-m]
V	Volume	[m^3]
V_d	Displaced volume	[m^3]
V_{dead}	Dead (clearance) volume	[m^3]
V_r	Volume ratio	[-]
$\dot{W}$	Work over a cycle	[W]
x_{dead}	Distance between piston and valve plate at TDC	[m]
x_p	Instantaneous compressor piston position	[m]
x_s	Compressor stroke	[m]

Greek Letters

β	Angle	[rad]

ϵ	Eccentricity of spring force	[m]
ε_{carnot}	Second law effectiveness	[-]
$\eta_{o,is}$	Overall isentropic efficiency	[-]
η_{vol}	Volumetric efficiency	[-]
ω	Frequency	[rad sec^{-1}]

Subscripts

BDC	Bottom Dead Center
cond	Condenser
cv	Control volume
evap	Evaporator
gas	Gas
leak	Leakage
sub	Subcooling
TDC	Top Dead Center

1. Introduction

A comprehensive simulation model for a miniature-scale linear compressor was developed by Bradshaw et al. (2011). The model predictions were validated using experimental results conducted on a prototype linear compressor constructed for the purpose. More recently, Bradshaw et al. (2012) used this model to study the sensitivity of the linear compressor to changes in various geometric parameters, which revealed that the linear compressor is highly sensitive to changes in the leakage gap between the piston and cylinder as well as the spring eccentricity; both parameters should be minimized for optimal performance. Therefore, it is important to quantify and control these parameters in any compressor design that is mass-produced to maximize performance. These studies further showed that it is advantageous to keep the stroke-to-diameter ratio relatively small. The disadvantage in using a small stroke-to-diameter ratio is the increase in leakage due to the increased leakage area. Therefore, a tradeoff exists between overall performance and leakage, which will depend strongly on the leakage gap between the piston and cylinder.

The previous studies also revealed that an increase in clearance (dead) volume between the piston and valve plate did not strongly influence the overall isentropic efficiency of the linear compressor. This suggested that a linear compressor could be utilized effectively for capacity control, but this hypothesis was not explored in detail.

Early investigations of a linear compressor were conducted by Cadman and Cohen (1969a,b) for traditional refrigeration systems. Cadman and Cohen observed that the free piston operation of this device created some peculiar effects such as piston drift, which poses practical challenges in the design of a single-acting linear compressor. Additional studies confirmed this behavior

(Pollak et al., 1979), while others proposed a double-acting design which provides a solution to this design challenge (Van der Walt and Unger, 1994. Unger and Novotny, 2002).

The opposing cylinders in the double-acting designs could capture the energy of the re-expanding gas, and were expected to allow the linear compressor to be used for efficient capacity control. Polman et al. (1980) developed a numerical model for a spring-less, double-acting, linear compressor. The overall efficiency of the compressor was found to be only weakly coupled to the stroke of the device as long as it was operated at the resonant frequency. The device could thus be operated efficiently with various mass flow rates.

Zhang et al. (2007) also realized this benefit of the linear compressor and developed a combination compressor/expander for a transcritical CO_2 refrigeration cycle. In this design, one cylinder of the linear machine acts as a compressor while the other replaces the expansion valve in the refrigeration cycle with a linear expander.

While the benefits of a double-acting machine are apparent, the unique free-piston design of a linear compressor suggests that some of these benefits can be captured using a single-acting design, as suggested by Bradshaw et al. (2012). The sensitivity analysis presented here examines the performance of a linear compressor with variable dead volume to simulate a variable-stroke compressor. These results are used to simulate a variable-capacity, miniature-scale refrigeration system for an electronics cooling application. In addition, the results are compared to thoses obtained with a traditional reciprocating compressor.

2. Dead (Clearance) Volume/Stroke Control

To simulate variable compressor capacity, the linear compressor model is operated with varying amounts of dead (clearance) volume (effectively, a variable-stroke operation), as depicted in Figure 1. The capacity of a linear compressor with a fixed cylinder size could be changed by changing the compressor stroke. However, since varying the stroke would also change the resonant frequency, it becomes difficult to isolate the effect of stroke length on compressor performance metrics, as the result is influenced by changes in both the stroke and the operating frequency (Bradshaw et al. 2012). Instead, an increasing compressor dead volume is used to represent a decreasing compressor stroke. The same piston diameter and stroke of 1.24 cm and 2.54 cm, respectively, are used as in the spring eccentricity and leakage gap studies presented in Bradshaw et al. (2012). This leads to a fixed displaced/swept volume for the compressor. The values of spring eccentricity, motor efficiency, and leakage gap are fixed at 0.5 cm, 0.9, and 3 μm, respectively. The dead volume in the compressor is varied from 10% to 120% of displaced volume. In addition, to assess the influence of friction, the dry friction coefficient, **f**, is varied between 0.1 and 0.3. The design conditions are the same as in Bradshaw et al. (2012): 20 ^{o}C, 40 ^{o}C, and 5 ^{o}C for evaporating, condensing, and superheat temperatures, respectively.

Figure 2 shows that the volumetric efficiency decreases linearly as the compressor dead volume is increased. With 0.3 cm^3 of dead volume the compressor operates at approximately 90% volumetric efficiency, while at 3.6 cm^3 dead volume the compressor operates at approximately 5% volumetric efficiency. Results for the three dry friction coefficients cannot be distinguished in Figure 2 as the volumetric efficiency is only very weakly dependent on friction.

The overall isentropic efficiency is also explored as shown in Figure 3. At a dead volume of 0.3 cm^3 for each dry friction coefficient, the efficiency is maximized. The overall isentropic efficiency decreases slightly until a dead volume of roughly 2.5 cm^3, beyond which the overall isentropic efficiency degrades rapidly. It is also noted that as the dry friction coefficient decreases, the overall performance increases.

These results show that a linear compressor behaves differently from a typical positive displacement compressor. The observed trend in the volumetric efficiency is a result of the decay in the amount of mass flow rate provided by the compressor as the dead volume increases. This decrease in volumetric efficiency is because the volume required to compress a fixed mass of gas changes. This means that a larger change in volume is required for the gas in the compression chamber to reach discharge conditions. In the case of a linear or reciprocating compressor this would result in a delay in when the gas would begin to discharge. This phenomenon can be explained by examining an idealized polytropic compression process, and introducing an expression for total volume which includes the dead volume:

$$V_r = \left(\frac{P_2}{P_1}\right)^{1/n} + \frac{V_{dead}}{\pi\left(D_p/2\right)^2 x_{TDC}}\left[\left(\frac{P_2}{P_1}\right)^{1/n} - 1\right] \quad (1)$$

where V_r is the volume ratio, the ratio of maximum to minimum compression volume:

$$V_r = \frac{A_p x_{BDC}}{A_p x_{TDC}} = \frac{x_{BDC}}{x_{TDC}}. \quad (2)$$

and x_{TDC} and x_{BDC} are defined as the piston position at the closest position to the discharge valve and the position furthest from the discharge valve, respectively, as shown in Figure 1.

Equation (1) shows that as the dead volume increases from zero (dead volume cannot be less than zero), the volume ratio required to obtain a certain pressure rise increases proportionally. Therefore, for a fixed volume and pressure ratio, the mass flow rate obtained will decrease proportionally as the dead volume increases.

The overall isentropic efficiency may be expected to follow a similar trend. However, as seen in Figure 3, the trend is not linear. As the dead volume increases from 0.3 cm^3 to roughly 2.5 cm^3, the overall efficiency shows only minor degradation. Figure 2 shows that the mass flow rate, on the other hand, is drastically reduced with the same change in dead volume. It may be concluded that the compressor produces less mass flow rate at the higher dead volume, but also requires less power input. This behavior can thus be exploited in considering the system-level performance, as discussed in the following section.

3. Capacity Control

A reduction in mass flow rate translates into a reduction in refrigeration capacity. By analyzing the refrigeration system for electronics cooling shown in Figure 4 the system cooling capacity may be calculated as follows:

$$\dot{Q}_{cool} = \dot{m}(h_1 - h_4). \quad (3)$$

If the system operates under fixed environmental conditions the enthalpies entering and exiting the system evaporator (h_4 and h_1) will remain constant, where h_4 is calculated assuming an isenthalpic throttling process:

$$h_4 = h_3 = h(T = T_{sat} - \Delta T_{sub}, P_2) \tag{4}$$

and ΔT_{sub} is assumed to be 10 °C. This means that the system cooling capacity is proportional to the mass flow rate generated by the compressor. The power required to drive the compressor is calculated using the comprehensive linear compressor model, and the system Coefficient of Performance (COP) is defined as:

$$COP = \frac{\dot{Q}_{cool}}{\dot{W}_{in}}. \tag{5}$$

where the power input is calculated as a combination of motor heat loss and force applied to the piston, as follows:

$$\dot{W}_{in} = \left(F_{drive}\right)_{rms}\left(\dot{x}_p\right)_{rms} + \dot{Q}_{motor}\,. \tag{5}$$

The driving force from the motor (F_{drive}) is assumed to be sinusoidal, the piston velocity ($\dot{x}_p$) is calculated based on the nonlinear vibration model given in Bradshaw et al. (2011), and the motor heat transfer is calculated by assuming a motor efficiency. In this work, the motor efficiency is assumed to be 90%.

For relative comparison to a reversible refrigeration cycle, the COP of a Carnot refrigeration cycle is utilized:

$$COP_{carnot} = \frac{T_{evap}}{T_{cond} - T_{evap}}. \quad (6)$$

Using the Carnot COP the second law effectiveness of the refrigeration cycle is defined as:

$$\varepsilon_{carnot} = \frac{COP}{COP_{carnot}}. \quad (7)$$

Using the results from Section 2 as an input with a dry friction coefficient of 0.1, a variable capacity system may be simulated, with a variable mass flow rate achieved by increasing the compressor dead volume. Figure 5 shows the predicted system COP and second law effectiveness ε as a function of the cooling capacity.

At the smallest cooling capacity the linear compressor produces the smallest mass flow rate, which translates to the largest dead volumes in Figure 2 and Figure 3. As the dead volume decreases the mass flow rate increases which results in an increase in cooling capacity. In addition, the overall isentropic efficiency of the compressor also increases as the dead volume decreases, which generates a better system COP. Figure 5 shows that a linear compressor can provide a reasonably high system COP in an electronics cooling system over a wide range of cooling capacities. This simulated compressor operates relatively well for cooling capacities from roughly 200 W to 600 W, which provides a sufficient amount of variation to maintain consistent cooling for a typical personal computer system, based on the predictions from the International Roadmap of Semiconductors (2011 ed.). This is another useful feature, besides the scalability and the low number of parts, of the linear compressor for an electronics cooling application.

A linear compressor also provides a straightforward mechanism for performing capacity control by modulating the input voltage to the linear motor. The input power to a single-phase linear motor can be expressed as:

$$\dot{W}_{in} = V_{in} I_{in} \cos\phi \tag{8}$$

where V_{in} is the input voltage, I_{in} is the current, and ϕ is the phase angle between the two. From Equations (5) and (8) it can been shown that $F_{drive} \propto V_{in}$, and from Bradshaw et al. (2011) that $F_{drive} \propto x_p$. Therefore, it can be concluded that $x_p \propto V_{in}$ which suggests that the stroke of the compressor, as well as system cooling capacity, can be efficiently controlled by adjusting (i.e. controlling) the input voltage to the linear motor.

4. Comparison of a Linear Compressor to Reciprocating Compressor Behavior

The unique behavior of a linear compressor shown in the previous sections is now compared to the more well-known reciprocating compressor technology. A reciprocating compressor provides a good benchmark for comparison to a linear compressor since the compression mechanism of the two devices may be readily compared. Fundamentally, linear and reciprocating compressors are very similar as they are both piston-cylinder devices. However, due to the kinematics of a reciprocating compressor the displaced volume is dictated by the design of the compressor and is not a function of the operating conditions or power input. Figure 6 shows a kinematic diagram of a reciprocating compressor driven with torque T at rotational speed ω.

Assuming that the compressor components act as rigid bodies, an expression for the motion of the piston as a function of the crank angle may be written as:

$$x_p = L_1 \cos(\beta_1) + \sqrt{L_2^2 - L_1^2 \sin^2(\beta_1)}. \tag{9}$$

Differentiating this expression twice, an expression for the acceleration of the piston is obtained:

$$\ddot{x}_p = -L_1 \omega^2 \cos(\beta_1) - \frac{L_1^2 \omega^2 \cos(2\beta_1)}{\sqrt{L_2^2 - L_1^2 \sin^2(\beta_1)}} - \frac{L_1^4 \omega^2 \cos(2\beta_1)}{2\sqrt[3]{L_2^2 - L_1^2 \sin^2(\beta_1)}}. \tag{10}$$

Additionally, an expression for the equation of motion of a reciprocating compressor may be constructed using the free body diagram given in Figure 6:

$$\underbrace{M_{mov}\ddot{x}_p}_{\text{Intertia}} + \underbrace{\mathbf{f}F_2 \sin(\beta_2)}_{\text{Damping}} + \underbrace{k_{gas} x_p}_{\text{Stiffness}} = F_2 \cos(\beta_2) \tag{11}$$

and noting that

$$k_{gas} \mathrm{x}_p \ = \ \mathrm{P}_{cv} \mathrm{A}_P. \tag{12}$$

This equation shows that a reciprocating compressor displays a similar equation of motion compared with the piston of a linear compressor given by Bradshaw et al. (2011) as

$$\underbrace{M_{mov}\ddot{x}_p}_{\text{Inertia}} + \underbrace{c_{eff}\dot{x}_p}_{\text{Damping}} + \underbrace{(k_{gas} + k_{mech})x_p}_{\text{Stiffness}} = k_{mech}\epsilon\theta + F_{drive} \tag{13}$$

$$J_{CG}\ddot{\theta} + k_{mech}\epsilon^2\theta = k_{mech}\epsilon x_p \tag{14}$$

Equations (13) and (14) show the two-degree-of-freedom equations of motion for a linear compressor piston and highlight the inertial, damping, and stiffness terms. The reciprocating compressor operation is also governed by inertial, damping, and stiffness terms. However, unlike a linear compressor, a reciprocating compressor has a stiffness that is only associated with the gas compression and thus, is much smaller than for a linear compressor (*i.e.*, $k_{linear} >> k_{recip}$). This small stiffness term makes it very difficult to operate a reciprocating compressor at a resonant frequency as it would require operation at a slower speed than at which A/C rotary motor technology typically operates (30 - 60 Hz). In addition, the leakage in a compressor is adversely impacted by the result of slowing operational speed, which is another reason why operating at lower speeds is typically avoided. Equation (11) is further expanded to determine the required torque from the crank. Realizing that β_2 can be written in terms of β_1 as

$$\tan\beta_2 = \frac{\left(L_1/L_2\right)\sin\beta_1}{\sqrt{1-\left[\left(L_1/L_2\right)\sin\beta_1\right]^2}}, \tag{15}$$

the torque required for piston movement may be calculated by solving the equation of motion described in Equation (11) for F_2 and using geometry to solve for the torque at the crank:

$$\mathbf{T} = (1+\mathbf{f})\left[(M_{mov}\ddot{x}_p + k_{gas}x_p)x_p \tan\beta_2\right]. \tag{16}$$

The power required to drive the reciprocating compressor is then given as:

$$\dot{W}_{in,recip} = T\omega. \tag{17}$$

The overall isentropic efficiency of the reciprocating compressor may then be expressed as:

$$\eta_{o,is,recip} = \frac{\dot{m}(h_{2,s} - h_1)}{\dot{W}_{in,recip}}. \quad (18)$$

Using these calculations, a direct performance comparison between a reciprocating and a linear compressor may be made. This is accomplished by simulating a compressor and calculating the work input using Equation (17) for the reciprocating compressor and using the methods described by Bradshaw et al. (2011) for the linear compressor. The same numerical solvers and solution approach are used for both simulations. These approaches are comprehensive and account for leakage past the cylinder, heat transfer, and valve dynamics. The reciprocating compressor simulation uses the presented kinematic analysis to calculate piston position and cylinder volume while the linear compressor uses the dynamic analysis presented in Bradshaw et al. (2011). With respect to leakage, a linear compressor is similar in behavior to a reciprocating compressor and the same leakage behavior is assumed for both machines. The major leakage in a piston-cylinder compressor occurs between the piston and cylinder and is modeled as an isentropic compressible flow of a gas through a nozzle. For the sake of comparison, the frictional losses are also considered to be identical for both the linear and reciprocating compressors. The frictional losses are modeled as dry friction between the piston and cylinder with a friction coefficient **f** of 0.1. Although the reciprocating compressor would have additional friction between the crank and connecting rod, this friction is not considered here to facilitate a more direct comparison of the two technologies. The sensitivity studies presented in Bradshaw et al. (2012) are not reproduced here with reference to reciprocating compressor performance. However, changes with respect to dead volume, or capacity control, are explored as this represents one of the significant differences between the two compressor types.

The variation in dead volume for the reciprocating compressor analysis matches that of a linear compressor. It is observed that the volumetric efficiency follows the same trend for both compressors. Therefore, the trends predicted in Figure 2 are realized for both compressors as each tends to lose mass flow as dead volume increases for the reasons explained in Section 2. However, when comparing the overall isentropic efficiency, Figure 7 shows that as the dead volume increases, the overall isentropic efficiency of a reciprocating compressor tends to decrease linearly, in a similar fashion as its volumetric efficiency.

The reason for the difference is noted in the equations of motion for the two compressors (Equations (13) and (11)), where the stiffness term in the linear compressor is much larger due to the mechanical springs. The stiffness in a mechanical system is analogous to capacitance in an electrical system, and provides a mechanism for a mechanical system to store energy. Therefore, the linear compressor has a higher ability to store energy, or mechanical capacitance. This proves useful when the compressor operates with a variable stroke (or with variable dead volume) as the linear compressor can recapture energy imparted to the gas. The trend observed in the overall isentropic efficiency of a reciprocating compressor is a result of the fact that the power required to drive the compressor mechanism remains relatively constant, but the net mass flow rate delivered decreases as the dead volume increases. In contrast, the linear compressor still shows the same reduction in mass flow rate as the reciprocating compressor; however, as a result of the large mechanical capacitance, the linear compressor is able to recapture some of the power typically lost during gas re-expansion and thus, operate at a lower power input at smaller capacity levels (*i.e.*, partial load).

5. Conclusions

This work demonstrates the ability of a linear compressor to recapture energy typically lost during the re-expansion process of a compressed gas. This ability gives the linear compressor the unique ability to operate efficiently over a wide range of dead (clearance) volumes. This ability may be utilized for capacity control in a miniature-scale refrigeration system for electronics cooling and other emerging applications, which call for a certain degree of capacity control. In addition, the small numbers of moving parts in the linear compressor, along with its insensitivity to dead volume, make it an ideal technology for electronics cooling applications.

6. Acknowledgement

The authors acknowledge support for this work from members of the Cooling Technologies Research Center, a National Science Foundation Industry/University Cooperative Research Center at Purdue University.

7. References

Bradshaw, C.R., Groll, E.A., Garimella, S.V., 2011. A comprehensive model of a miniature-scale linear compressor for electronics cooling. Int. J. Refrigeration, 34(1), pp.63-73.

Bradshaw, C.R., Groll, E.A., Garimella, S.V., 2012. A Sensitivity Study of a Miniature-Scale Linear Compressor for Electronics Cooling using a Comprehensive Model. Int. J. Refrigeration, (in-press).

Cadman, R., Cohen, R., 1969a. Electrodynamic oscillating compressors: Part 1 design based on linearized loads. ASME J. Basic Eng December, 656–663.

Cadman, R., Cohen, R., 1969b. Electrodynamic oscillating compressors: Part 2 evaluation of specific designs for gas load. ASME J. Basic Eng. December, 664–670.

Pollak, E., Soedel, W., Cohen, R., Friedlaender, F., 1979. On the resonance and operational behavior of an oscillating electrodynamic compressor. J. Sound Vib. 67, 121–133.

Polman, J., De Jonge, A.K., Castelijns, A., 1980. A Capacity Controlled Free-Piston Electrodynamic Compressor. XV International Congress of Refrigeration: Comission B2. 3(2).

Unger, R., Novotny, S., 2002. A high performance linear compressor for cpu cooling. In: Proceedings of the International Compressor Engineering Conference, Purdue University, West Lafayette, IN, USA. No. C23-3.

Van der Walt, N., Unger, R., 1994. Linear compressors-a maturing technology. In: Proceedings of the International Compressor Engineering Conference, Purdue University, West Lafayette, IN, USA. pp. 239–246.

Zhang, B., Peng, X., He, Z., Xing, Z., Shu, P., 2007. Development of a Double-Acting Free-Piston Expander for Power Recovery in Transcritical CO2 Cycle. App. Therm. Eng. 27(8). 1629-1636.

List of Figures

Fig1-schematic.eps

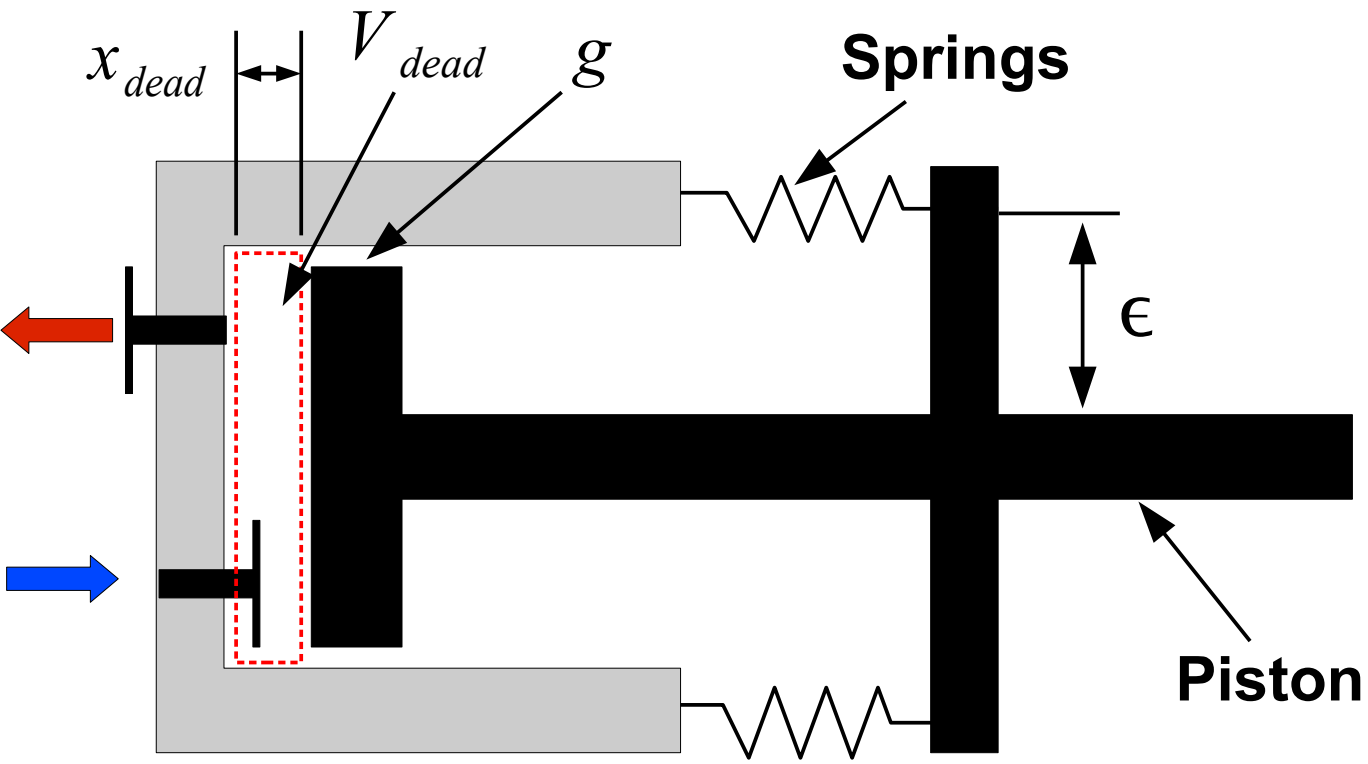

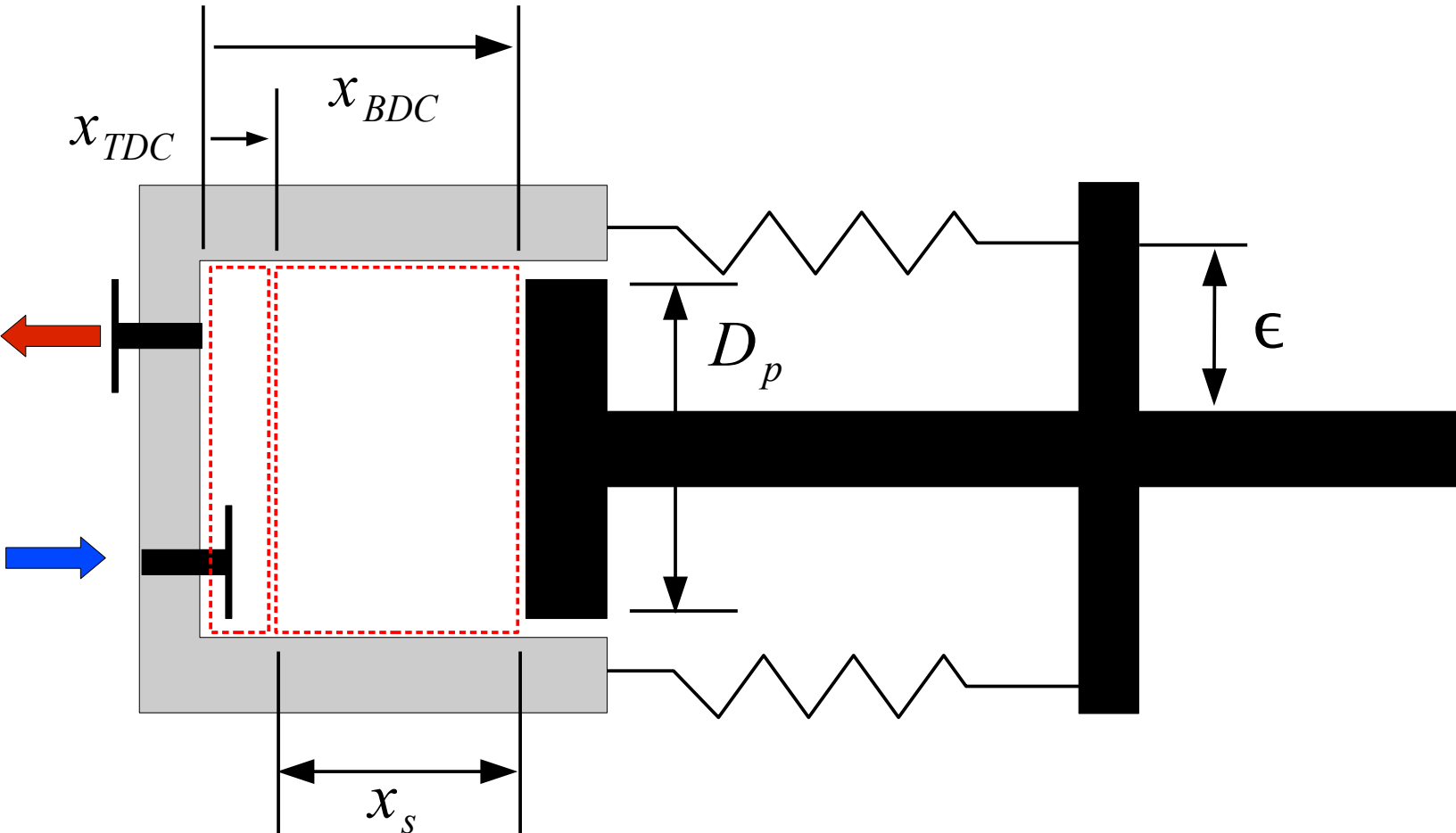

Fig2-volume_v.eps

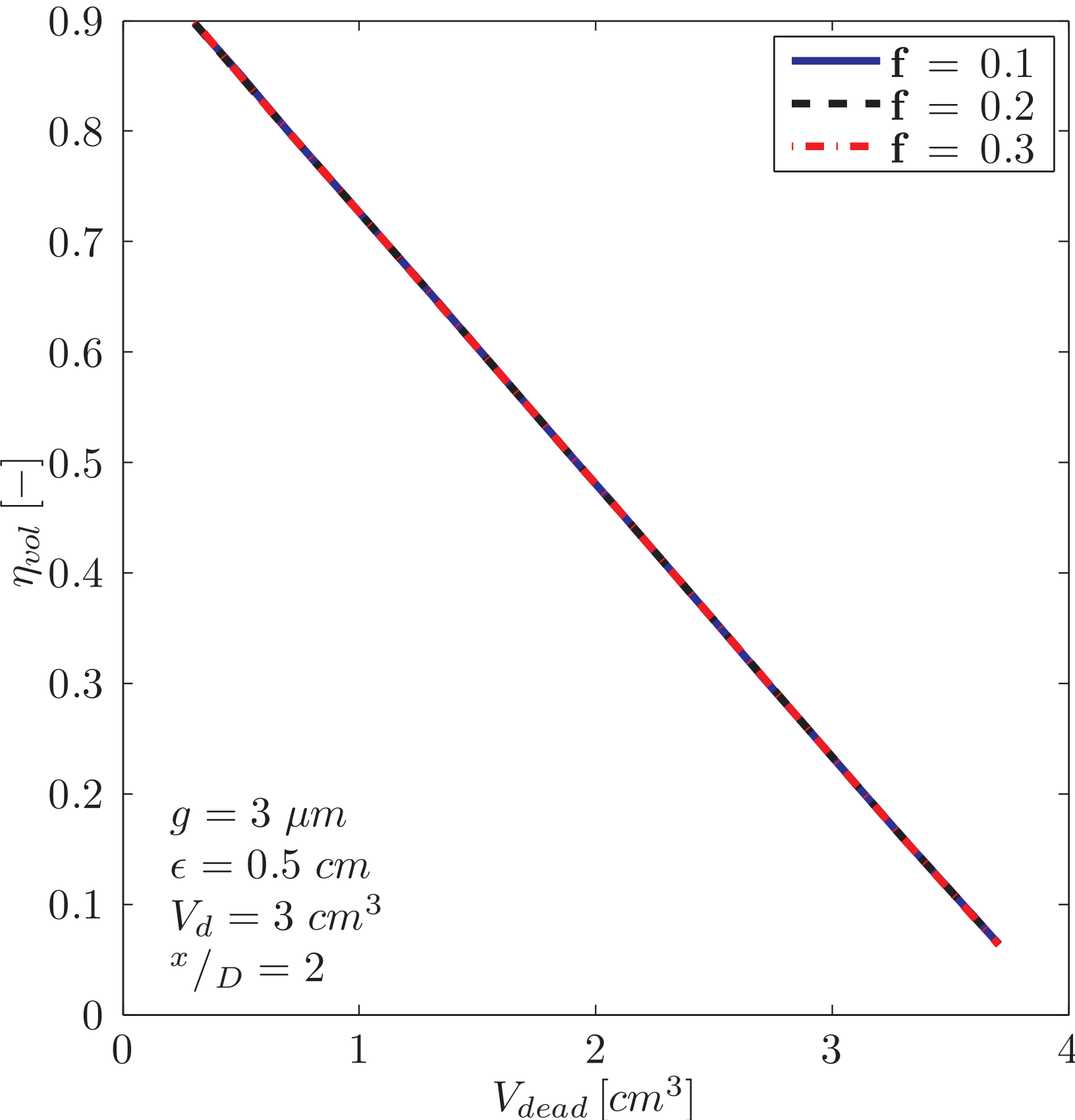

Fig3-overall_v.eps

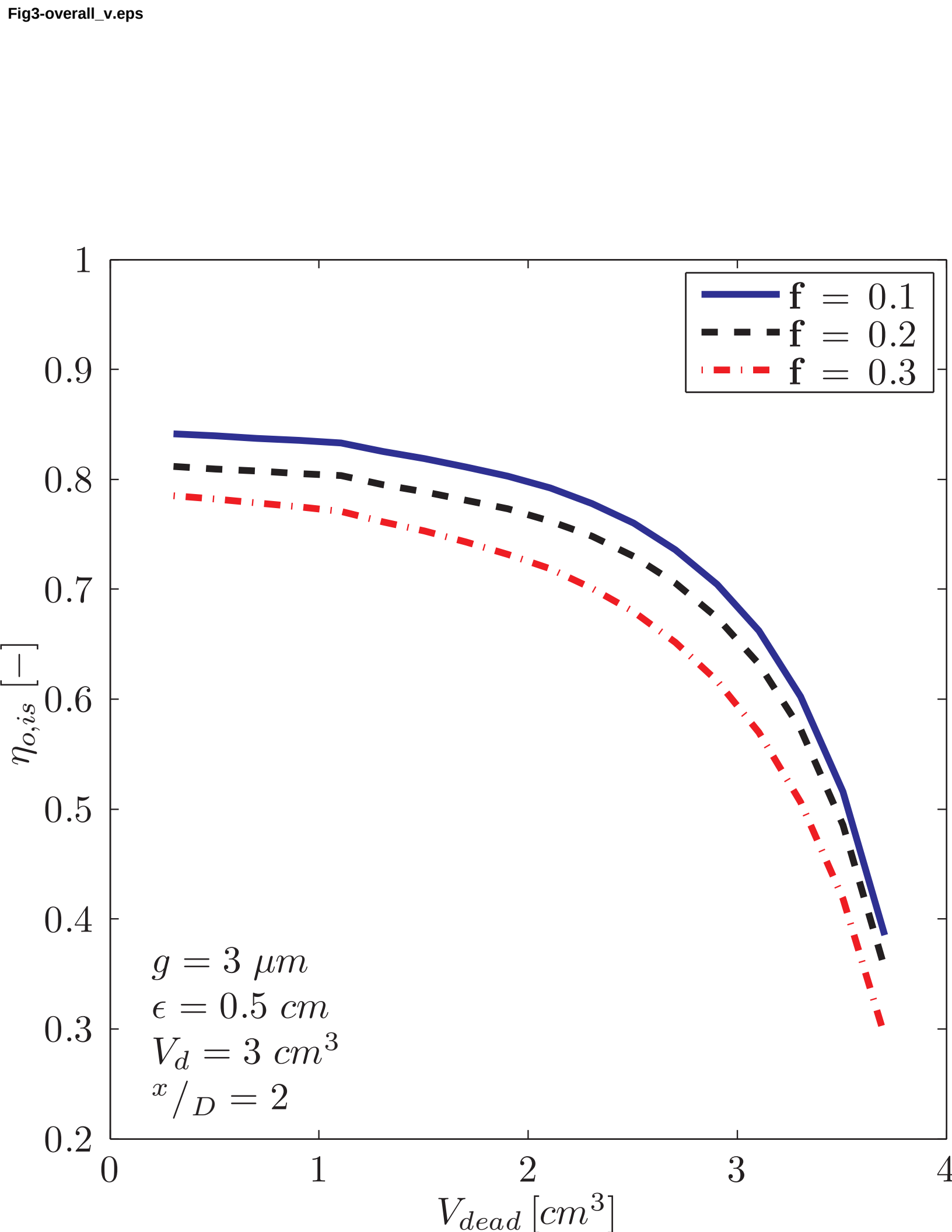

Fig4-cycle.eps

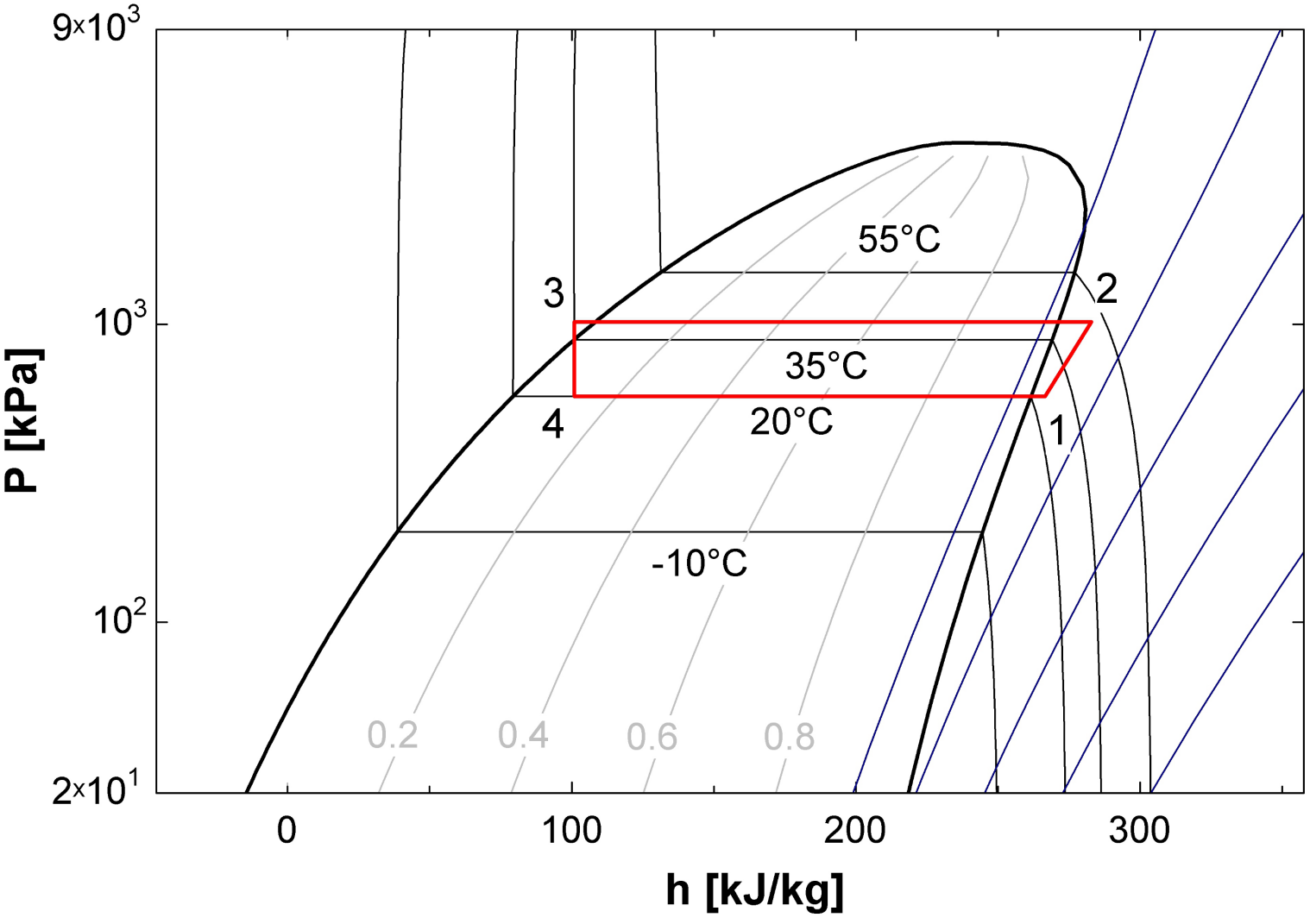

Fig5-COP.eps

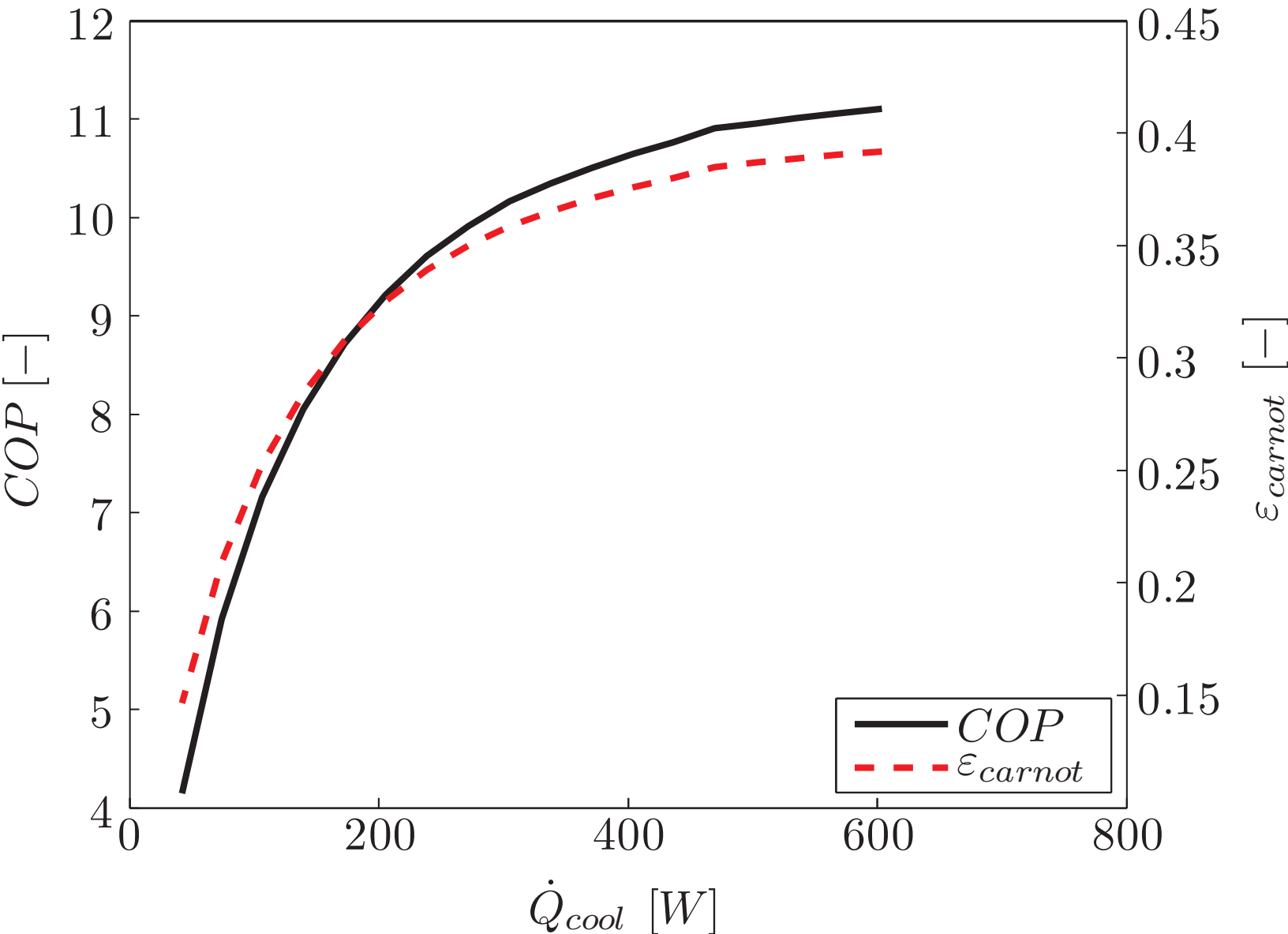
12
11
10
9
8
7
6
5
4
0
200
400
600
800
0.45
0.4
0.35
0.3
0.25
0.2
0.15
COP [–]
ε_{carnot} [–]
$\dot{Q}_{cool}$ [W]
COP
ε_{carnot}

Fig6-recip.eps

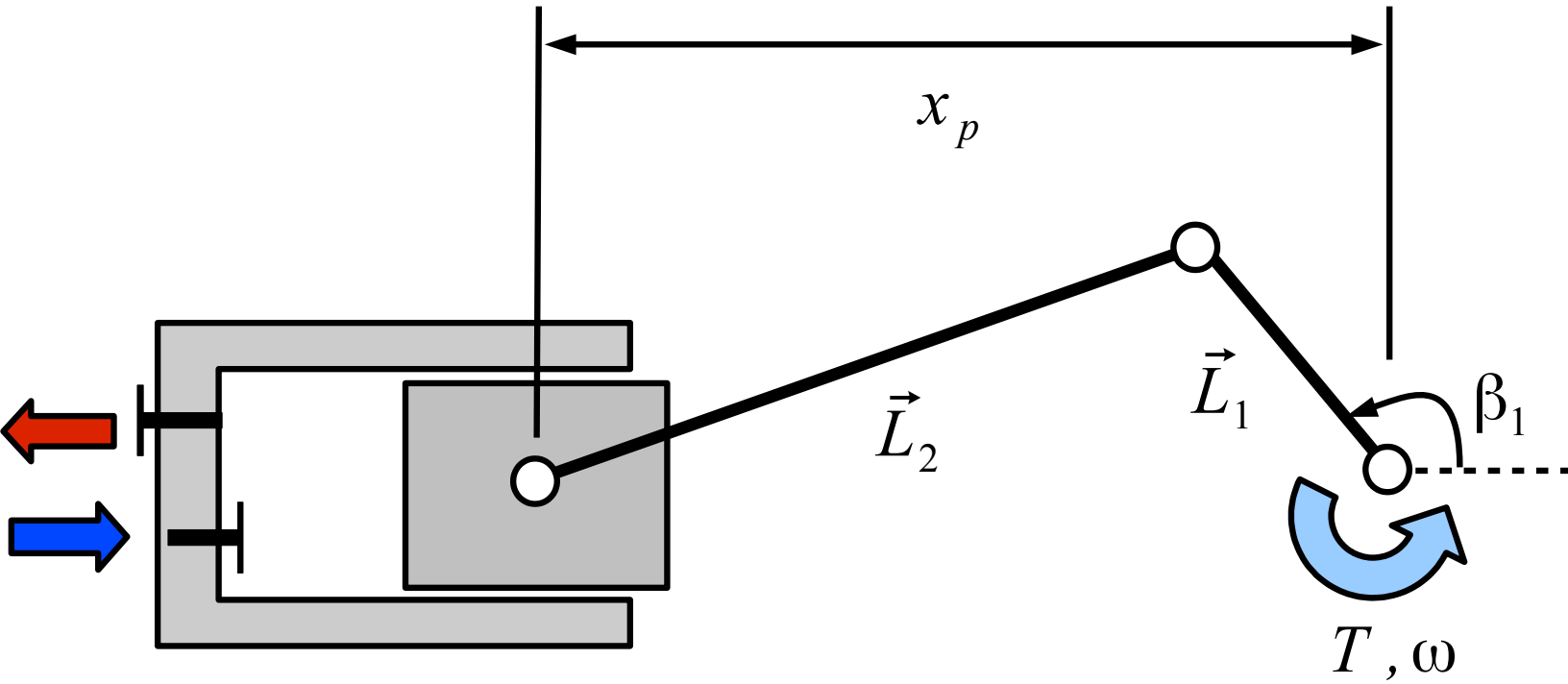

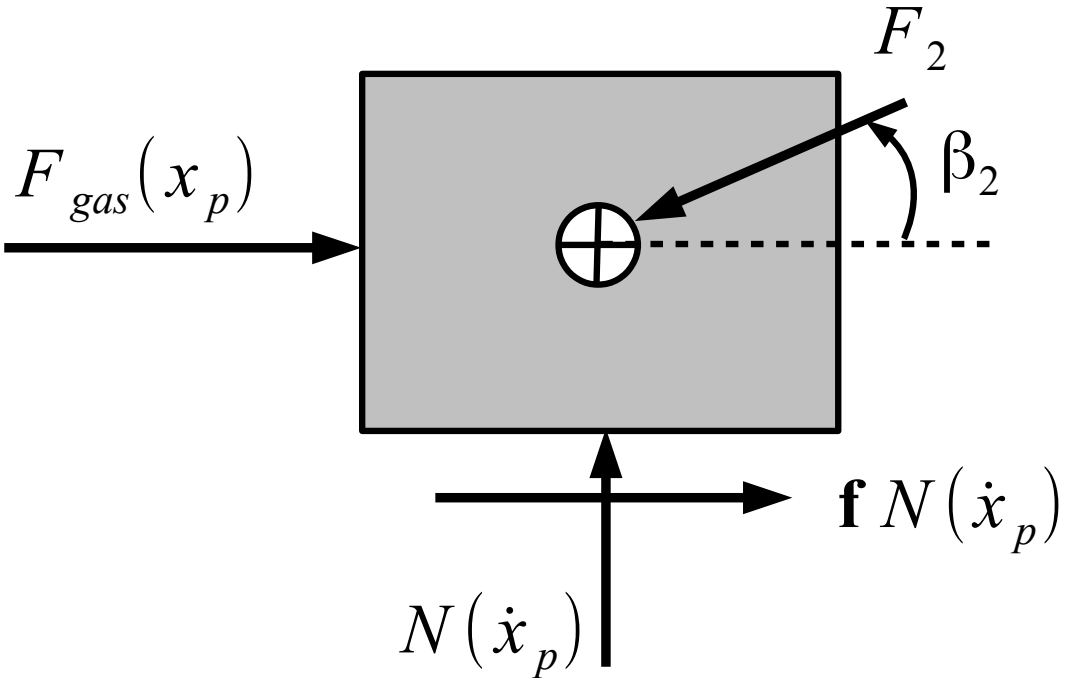

Fig7-overall_v_r.eps